WPPMI-PR(17) 17847

R.M. Mozzillo et al.

Structural assessment on DEMO Lower Port Structure

Preprint of Paper to be submitted for publication in
Fusion Engineering and Design

This work has been carried out within the framework of the EUROfusion Consortium and has received funding from the Euratom research and training programme 2014-2018 under grant agreement No 633053. The views and opinions expressed herein do not necessarily reflect those of the European Commission.

Structural assessment on DEMO Lower Port Structure

Rocco Mozzillo[a], Christian Bachmann[b], Giuseppe Di Gironimo[a],

[a] *CREATE, University of Naples Federico II, DII, P.le Tecchio 80, 80125, Naples, Italy*
[b]*EUROfusion PMU, Boltzmannstraße 2, 85748 Garching, Germany*

The present work focuses on structural assessment of DEMO Vacuum Vessel structure. Since previous studies have been addressed the structural scheme of the main vessel, the layout of vessel supports, the position of the pumping port cut and different inclinations of the lower port have been addressed. All design configurations have been analysed according to RCC MRx. The structure was checked against a vertical load due to a Vertical Displacement Event in combination with the estimated mass of all components supported by the vessel. The outcome of the assessment gives relevant information about the optimal position of the supports, the impact of the pumping port duct cut and the lower port inclination.

Keywords: DEMO, Vacuum Vessel, Elasto-plastic analysis, FEM.

1. Introduction

The DEMO Vacuum Vessel (VV) is a large torus structure that contains and supports the in-vessel components (such as breeding blanket and divertor cassette). The VV is part of the primary confinement barrier for the reactor and shall be designed to withstand the electromagnetic loads during plasma disruptions and design basis accidents. The most critical disruption events are the vertical displacement events (VDE) which are uncontrolled vertical motion of the plasma column in tokamaks that brings it in contact with the surrounding structures. The expected vertical load due to a VDE becomes one of the first design load to consider when designing the vacuum vessel of a tokamak.

To verify the structural integrity of the VV according to RCC-MRx code [1], three different types of damages shall be evaluated:

- P type damage
- S type damage
- Buckling (with manufacturing imperfection)

In the present study just the "P type damage" has been evaluated. A VDE is indeed an event of Category 3 and the Level C criteria must be applied [2]. According to RCC-MRx in this case fatigue analyses are not required, while the buckling phenomena will be studied in more detailed design phase when more detailed design of VV will be available. The analysis has been run according to the elastoplastic procedure. Indeed in the elastoplastic analysis procedure the load is applied progressively to the deformed structure up to plastic collapse. Minimum true stress-strain material properties is considered and required collapse load factor is 2.0 (i.e. RCC- MRx RB 3251.12) [1].

Previous studies on DEMO 2014 configuration [3][4] addressed the structural scheme of the main vessel. The aim of the present paper is indeed to provide:

- ✓ a structural assessment of the VV structure updated to DEMO 2015 configuration model [5] subjected to a VDE (Fig. 1);
- ✓ a structural assessment of different configurations of VV structure in terms of lower port inclination, supports and pumping port cut positions.

The assessment is based on finite element method (FEM) that is being discussed in the next sections. In particular, according to RCC MRx – RB 3242 "Elastoplastic analysis of a structure subjected to a monotonic loading", the VV has to be verified against the maximum vertical load due to a VDE, as well as its own weight. Therefore the weight of all the components that are not modelled is considered as well in the calculation.

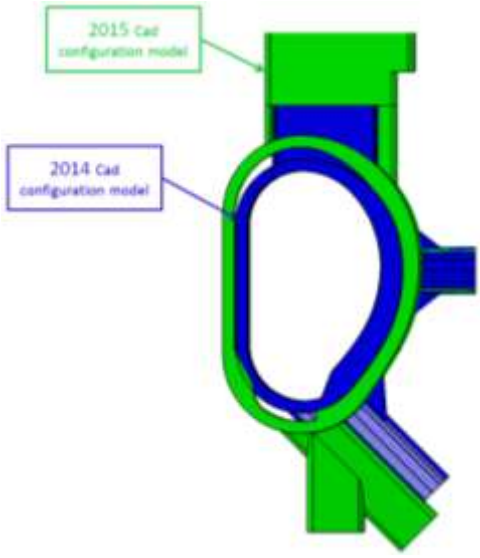

Fig. 1 Comparison between 2014 and 2015 DEMO VV shape

author's email: rocco.mozzillo@unina.it

2. Vacuum Vessel structure and design configurations

Since a previous assessment [4] on the structural scheme of the VV confirmed its capability to withstand the loads due to a critical VDE [2], this scheme has been adopted also in DEMO 2015 design. The DEMO VV is a double-walled structure made from SS 316 L (N). Its overall thickness of 0.60–1.15 m is formed by inner and outer shells, 60 mm in thickness, joined by welded stiffening ribs of 40mm in thickness. In the current configuration [5] the VV is divided toroidally into 18 sectors (20° for each one) which are joined by field welding. The lower port is joined to the main vessel structure and is reinforced by gusset plates (Fig. 2).The poloidal ribs aligned with the gussets plates are 80 mm in thickness. Since previous studies [4] confirmed that the gussets plates are critical components their thickness is set at 100mm. This choice guarantees the structural continuity in order that loads can be safely exchanged between ports and main vessel [6]. Moreover the ribs are as near as possible to the center line of the five Breeding Blanket Sectors.

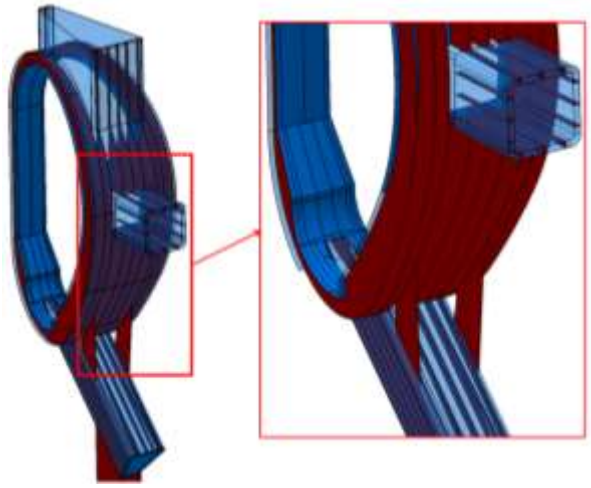

Fig. 2 Surface model of DEMO VV 2015

The outboard shells of VV are faceted in toroidal direction in order to assure the single curvature of the surfaces, while they have double curvature on the top and bottom area at inboard side.
Since the present assessment investigates the supports layout and its impact on VV structure, they have been just sketched with different layout configurations since their design is not in the scope of the present study. Each support is joined to the correspondent port sidewall and has a length of 2 meter along the radial direction.

2.1. Design Configurations

In order to assess the limits of the VV supports position, the lower port inclination and the pumping duct position, 36 different configurations of the DEMO VV single sector have been analyzed according to [1]. Three different support layouts (midline of supports at 9, 12 and 15 meters from the tokamak axis), four different inclination of the lower port (inclined of 0°, 10°, 30°, 45° with respect to the tokamak equatorial plane) and two positions for the pumping port cut (at about 9 and 11 meters from the tokamak axis, named respectively "*pd option 1*" and "*pd option 2*") have been combined to obtain all configurations to be analyzed (Fig. 3).

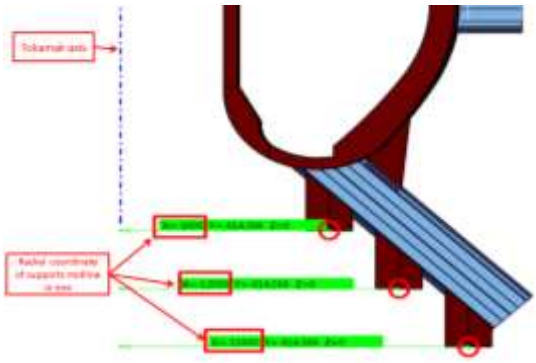

Fig. 3 Vacuum Vessel Supports Layout

A CAD model of the VV structure has been developed for each configuration (Fig. 4). In order to allow a direct comparison of the FE analysis results, all gussets plates have been conceived with the same cross section. As aforementioned the variables used to define each configuration were:

- ✓ the lower port inclination
- ✓ the pumping duct cut position
- ✓ the lower port supports position

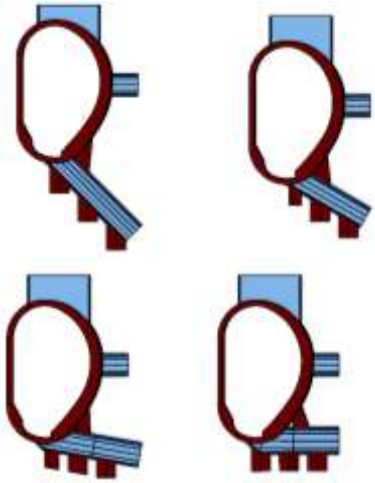

Fig. 4 CAD surface models of DEMO 2015 configurations

The configurations have been properly named using an "*ID configuration*", their geometrical characteristics have been reported in Table 1.

Table 1 ID and characteristics of DEMO VV design configurations

ID of Demo VV Configurations	Radial Support Location [m]		
	9	12	15
45° - without pumping duct	L9_45	L12_45	L15_45
45° - pumping duct option 1	L9_45_pd_1	L12_45_pd_1	L15_45_pd_1
45° - pumping duct option 2	L9_45_pd_2	L12_45_pd_2	L15_45_pd_2
30° - without pumping duct	L9_30	L12_30	L15_30
30° - pumping duct option 1	L9_30_pd_1	L12_30_pd_1	L15_30_pd_1
30° - pumping duct option 2	L9_30_pd_2	L12_30_pd_2	L15_30_pd_2
10° - without pumping duct	L9_10	L12_10	L15_10
10° - pumping duct option 1	L9_10_pd_1	L12_10_pd_1	L15_10_pd_1
10° - pumping duct option 2	L9_10_pd_2	L12_10_pd_2	L15_10_pd_2
0° - without pumping duct	L9_0	L12_0	L15_0
0° - pumping duct option 1	L9_0_pd_1	L12_0_pd_1	L15_0_pd_1
0° - pumping duct option 2	L9_0_pd_2	L12_0_pd_2	L15_0_pd_2

3. Finite element model

Based on the CAD data, a FEM model has been developed for each configuration (Table 1). The CAD models have been developed using CATIA V5 by Dassault Systemes, while ANSYS Workbench has been used to run the FEM analyses.
The reference element type for the FE model is SHELL 181. The resulting mesh has about 120000 nodes and 125000 elements. In the next sections the FE model characteristics are described.

3.1. Design Loads

The VV was assessed for the load combination of a VDE and dead weight. This load combination is classified as a Category 3 event (Category 3 - Class C: Dead weight + VDEIII) [2].
The worst case occurs during a VDE slow-down [2], when the plasma exerts an overall vertical load of about 150 MN.

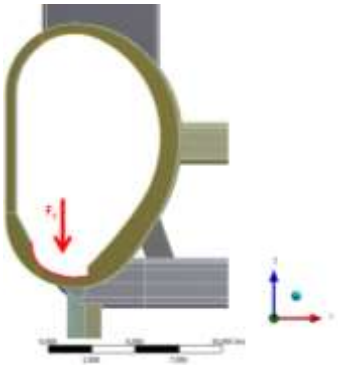

Fig. 5 Direction and verse of the load

With reference to the weight force, the estimated total mass for a DEMO sector [2], including port extensions, ducts, plugs, in-wall shielding, blanket modules, divertor modules is:

$$\mathbf{m_{single\ sector} = 1650\ tons} \quad (1)$$

However, since these components have not been modeled yet with the degree of accuracy needed for a significant FEM analysis, the density value of VV material has been chosen to take into account the actual weight force that the vessel has to bear (see section 3.2). The weight is hence uniformly distributed through the whole VV structure, but this approximation is acceptable for the purposes of the present study.

3.2. Materials

Two different material types have been defined in FE model. In order to account the desired behaviours the materials type have been customized starting from the reference material characteristics. Moreover the material property values are defined at the operating temperature of 200° C [7].

Table 2 Material properties at 200°C

Description	E [Pa]	ν	Density [kg/m^3]	Behaviour
Custom Stainless Steel	$1{,}93 \cdot 10^{11}$	0.3	40.920*	Elasto - plastic
High Stiffness steel	$1 \cdot 10^{16}$*	0.3	7.850	Linear Elastic

*artificial value

The "*Custom stainless steel*" was applied to the Vacuum Vessel and Port Structures (Table 2). As mentioned, an artificial density value of 40920 kg/m^3 has been assigned to this material to account for the masses of all the components that lay on the main vessel, yet not modelled, such as port extensions, plugs, in-wall shielding, blanket modules, divertor modules, etc. [2]. The material behaviour is elastoplastic. The minimum true stress-strain curve of the AISI 316 L(N) stainless steel [7] has been used for calculations.

The "High stiffness steel" is a custom material with an artificial modulus of elasticity that is five orders of magnitude greater than the real stainless steel. This means that it be considered as "infinitely stiff" with respect to the other material used for FEM modelling. This material was applied to the support plates of the VV to avoid their possible failure and to reduce singularity effects due to the restraints set up on them. This simplification is acceptable because the present study does not investigate supports structure but just their layout.

3.3. Boundary conditions

A planar symmetry condition has been placed on the two boundary edges of the VV sector (at -10° and +10°, respectively) (Fig. 6).

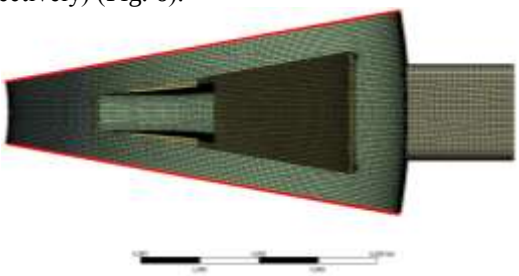

Fig. 6 Symmetry boundary conditions on the left and right edges of VV single sector

To allow rigid rotations the restraints have been placed just on one node at midline of each support plate (Fig. 7).

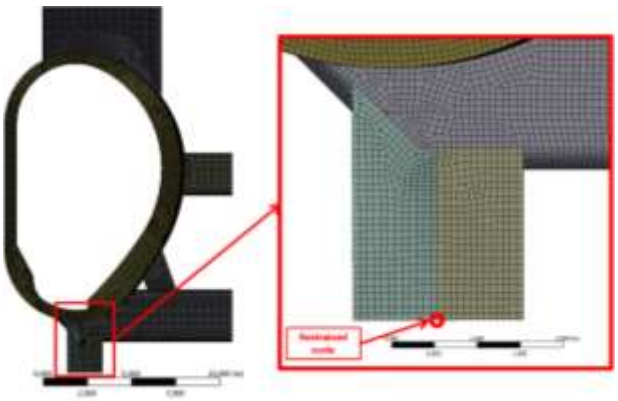

Fig. 7 Position of the restraints on the VV supports

The vessel support was constrained against rotation around the vertical axis and against translation along a direction inclined with respect to the vertical axis. A radial constraint cannot be implemented as it would constrain the thermal expansion of the VV.

4. Results

The results of the present assessment consist of 36 runs, one for each configuration (Table 1). Since the configurations with the supports at 15 meters does not meet MRx-2012 code [1], the configurations with the supports at 15 meters and pumping duct cut have not been run. These configurations are expected to have collapse load factors lower than the reference configuration (e.g. without pumping port cut and support radial location below 15 meters). All FEM models were checked to be consistent with the load condition through the calculation of the reaction forces. Since the load is increased in multiple load steps, the calculation diverges due to excessive plastic deformations (hereinafter referred to as "plastic instability"). The last load before the loss of convergence of the Newton-Raphson algorithm [8] is assumed as the actual collapse load.
In Table 2 are listed the load factors at collapse for each configuration.

Table 3 Results in brief and geometrical characteristics

ID Configuration	Lower port inclination	VV supports radial coordinate [m]	Pumping Duct		Last Converged Load Factor	Comments
			Radial Coordinate of the Pumping Duct Axis [m]	Main dimensions of Pumping Duct Cut [mxm]		
L9_45	45°	9	N/A	N/A	5.31	Lower port sidewalls affected by plastic instability at collapse
L9_45_pd_1			10,2	2,5x1,23	3.14	Lower port sidewalls affected by plastic instability at collapse
L9_45_pd_2			9,7	2,5x1,23	3.40	Lower port sidewalls affected by plastic instability at collapse
L12_45		12	N/A	N/A	2.59	Lower port gussets affected by plastic instability at collapse
L12_45_pd_1			10,2	2,5x1,23	2.55	Lower port gussets and sidewalls affected by plastic instability at collapse
L12_45_pd_2			9,7	2,5x1,23	2.64	Lower port gussets and sidewalls affected by plastic instability at collapse
L15_45		15	N/A	N/A	**1.36**	Lower port gussets affected by plastic instability at collapse
L15_45_pd_1			10,2	2,5x1,23	n/a	n/a
L15_45_pd_2			9,7	2,5x1,23	n/a	n/a
L9_30	30°	9	N/A	N/A	3.96	Lower port sidewalls affected by plastic instability at collapse
L9_30_pd_1			9,7	2,5x1	2.99	Lower port sidewalls affected by plastic instability at collapse
L9_30_pd_2			11,3	2,5x1	3.44	Lower port sidewalls affected by plastic instability at collapse
L12_30		12	N/A	N/A	3.20	Lower port gussets affected by plastic instability at collapse
L12_30_pd_1			9,7	2,5x1	3.10	Lower port gussets affected by plastic instability at collapse
L12_30_pd_2			11,3	2,5x1	3.00	Lower port gussets affected by plastic instability at collapse
L15_30		15	N/A	N/A	**1.42**	Lower port gussets affected by plastic instability at collapse
L15_30_pd_1			9,7	2,5x1	n/a	n/a
L15_30_pd_2			11,3	2,5x1	n/a	n/a
L9_10	10°	9	N/A	N/A	4.50	Lower port sidewalls affected by plastic instability at collapse
L9_10_pd_1			11,3	2,5x1	3.93	Lower port sidewalls affected by plastic instability at collapse
L9_10_pd_2			9	2,5x0,8	2.53	Lower port sidewalls affected by plastic instability at collapse
L12_10		12	N/A	N/A	2.48	Lower port gussets affected by plastic instability at collapse
L12_10_pd_1			11,3	2,5x1	3.24	Lower port gussets affected by plastic instability at collapse
L12_10_pd_2			9	2,5x0,8	2.53	Lower port gussets affected by plastic instability at collapse
L15_10		15	N/A	N/A	**1.15**	Lower port gussets affected by plastic instability at collapse
L15_10_pd_1			11,3	2,5x1	n/a	n/a
L15_10_pd_2			9	2,5x0,8	n/a	n/a
L9_0	0°	9	N/A	N/A	4.20	Lower port sidewalls affected by plastic instability at collapse
L9_0_pd_1			11,3	2,5x1,5	4.00	Lower port sidewalls affected by plastic instability at collapse
L9_0_pd_2			9	2,9x0,6	3.82	Lower port sidewalls affected by plastic instability at collapse
L12_0		12	N/A	N/A	3.50	Lower port gussets affected by plastic instability at collapse
L12_0_pd_1			11,3	2,5x1,5	3.47	Lower port sidewalls affected by plastic instability at collapse
L12_0_pd_2			9	2,9x0,6	4.22	Lower port gussets and sidewalls affected by plastic instability at collapse
L15_0		15	N/A	N/A	**1.77**	Lower port gussets affected by plastic instability at collapse
L15_0_pd_1			11,3	2,5x1,5	n/a	n/a
L15_0_pd_2			9	2,9x0,6	n/a	n/a

In all configurations except in the case with supports at 15 meters the required collapse load factor is met. The mechanisms of failure have been identified (Table 2), in detail the structure collapses due to:

- a plastic instability of the lower port gussets
- a plastic instability of the lower port sidewalls

In the following chapters is reported the *"equivalent plastic strain"* at collapse in three representative configurations.

4.1. Support at 9 meters

In the configuration "*L9_30_pd_2*", the joining area between the lower port and main vessel, at last converged step (the collapse load factor is 3.44), is subjected to high loads and high plastic deformation.
In detail the loads flows mainly in the main vessel structure and the gussets are partially unloaded. The collapse occurs on the port sidewalls. Unrealistic plastic deformations occur in the area between supports (with infinite stiffness) and lower port, this numerical phenomenon is due to the junction between components with different material type (Fig. 8).

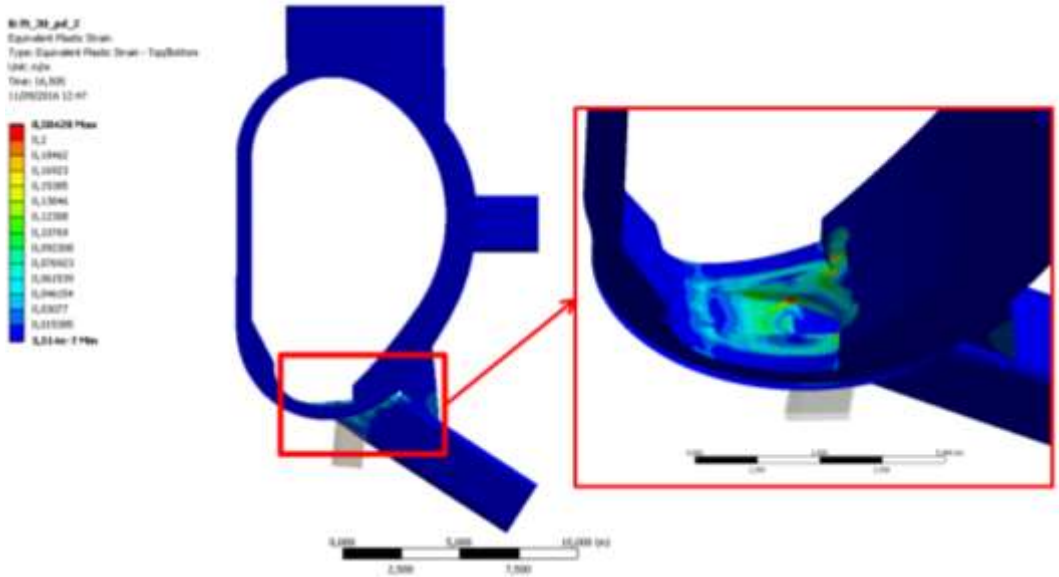

Fig. 8 Equivalent plastic strain at last converged step in the configuration with supports a 9 meters

4.2. Supports at 12 meters

In configuration "*L12_10*" , at collapse, the most critical components of the VV are the lower port gussets. Indeed at last converged step (the collapse load factor is 2.48) the gussets are subjected to plastic instability. In other words the collapse load factor gives a measure of how much load the gussets can withstand.

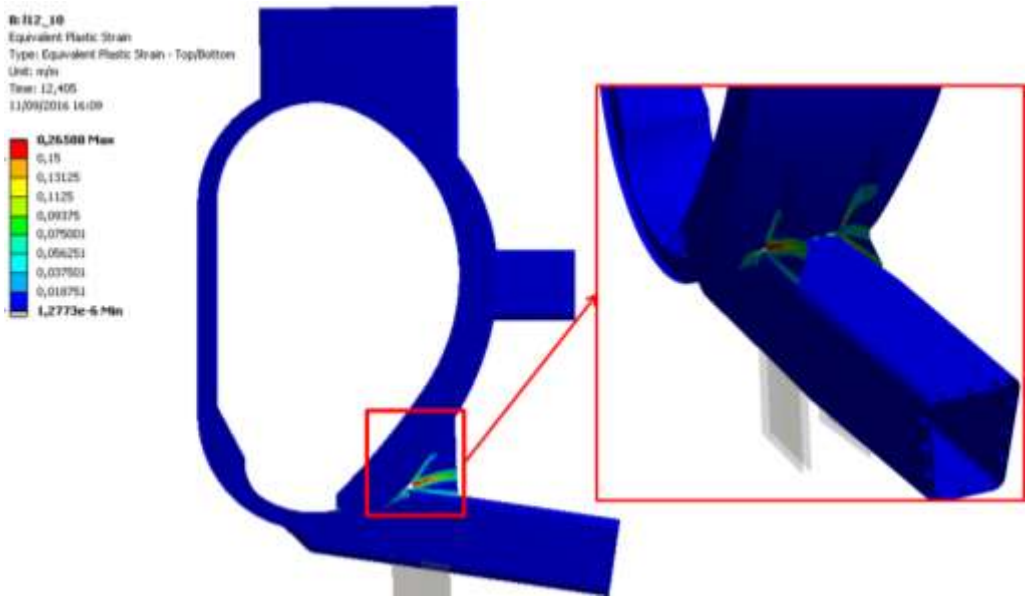

Fig. 9 Equivalent plastic strain in configuration with the support at 12 meters

4.1. Support at 15 meters

In "L15_45" the RCC MRx code are not meet, indeed the last converged load factor is lower than 2.0. As shown in Fig. 10, the collapse is on the lower port gusset plates. That plates at collapse are affected by a plastic instability phenomenon.

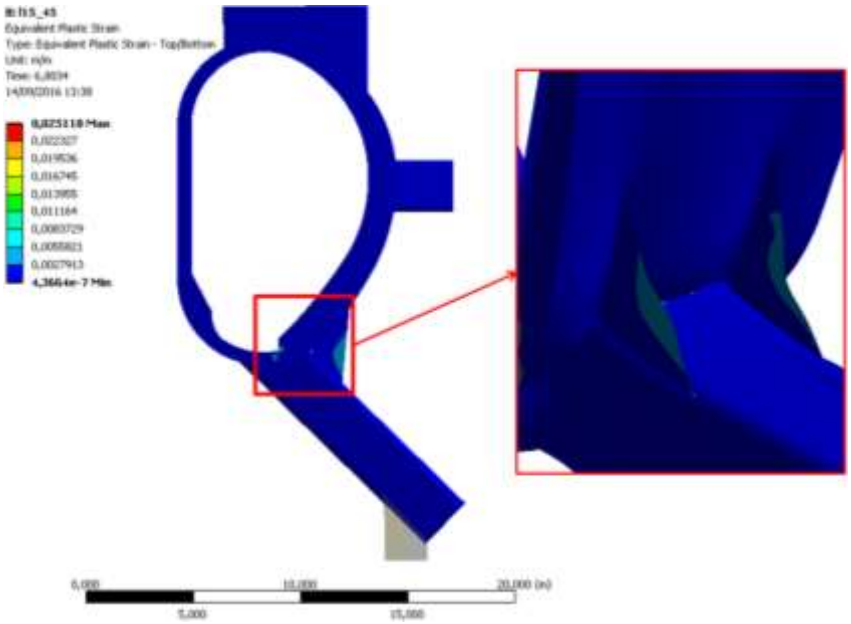

Fig. 10 Equivalent plastic strain in configuration with the support at 15meters

5. Conclusion

A FEM-based structural analysis has been conducted on the current design of DEMO VV [5]. The choice of using a FE shell model is acceptable and also provides conservative results since in all configurations the maximum plastic deformation at collapse is quite limited.

The behaviour of the updated structure of DEMO VV 2015 is similar to the previous configuration (e. g. 2014 configuration) (Fig. 11). In all configurations, except in the case of supports placed at 15 meters from the tokamak axis, the collapse load factor is higher than 2.0 (Table 3) as required by RCC-MRx code. The gussets were found to be the critical components. Moreover the present assessment confirms previous results about the internal structure of the vessel giving relevant information for future development of its design. The positions and dimensions of the pumping duct cut do not generate relevant changes in the stiffness of VV structures. The outcome of the study confirms that the trend of the load factor depends mainly on the radial coordinate of the supports (Fig. 11). The highest collapse load factor is reached in the configurations with the lowest radial coordinate.

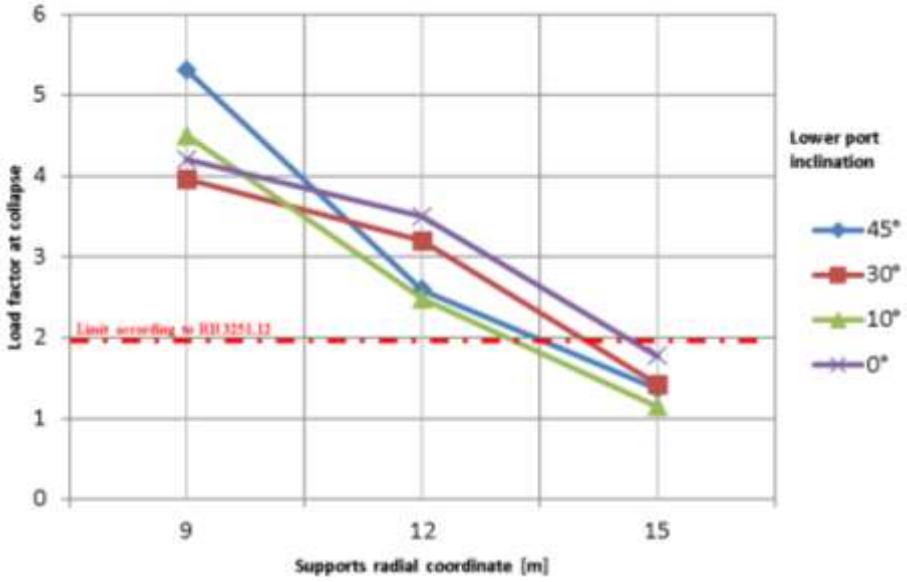

Fig. 11 Collapse Load factors in configurations without pumping port cut

In order to avoid the P type damage against a VDE, the supports should be placed between nine and twelve meters from the tokamak axis.

Acknowledgments

This work has been carried out within the framework of the EUROfusion Consortium and has received funding from the Euratom research and training programme 2014-2018 under grant agreement No 633053. The views and opinions expressed herein do not necessarily reflect those of the European Commission.

References

[1] RCC-MRx 2012, Design And Construction Rules For Mechanical Components Of Nuclear Installations 2012 Edition, Paris – France.

[2] C. Bachmann, W. Biel, S. Ciattaglia, G. Federici, F. Maviglia, G. Mazzone, G. Ramogida, F. Villone, N. Taylor. Initial definition of structural load conditions in DEMO. Proceedings of Soft 2016. Symposium on Fusion Technology, Prague, 05-09 September 2016

[3] Mozzillo, R., Marzullo, D., Tarallo, A., Bachmann, C., & Di Gironimo, G. (2016). Development of a master model concept for DEMO vacuum vessel. Fusion Engineering and Design.

[4] Mozzillo, R., Tarallo, A., Marzullo, D., Bachmann, C., Di Gironimo, G., Mazzone, G. (2016). Preliminary structural assessment of DEMO Vacuum Vessel against a Vertical Displacement Event. Fusion Engineering and Design

[5] M. Botond, DEMO TOKAMAK COMPLEX , 2M9AJJ

[6] G. Federici, R. Kemp, D. Ward, C. Bachmann, T. Franke, S. Gonzalez, C. Lowry, M. Gadomska, J. Harman, B. Meszaros, C. Morlock, F. Romanelli, R. Wenninger, Overview of EU DEMO design and R&D activities; Fusion Engineering and Design 89 (2014) 882–889.

[7] Appendix A to ITER SDC-IC, Materials Design Limit Data, Iter_222RLN

[8] P. Deuflhard, Newton Methods for Nonlinear Problems. Affine Invariance and Adaptive Algorithms. Springer Series in Computational Mathematics, Vol. 35. Springer, Berlin, (2004), ISBN 3-540-21099-7.